AJNR

Laboratory simulations and training in endovascular embolotherapy with a swine arteriovenous malformation model.

T F Massoud, C Ji, F Vinuela, F Turjman, G Guglielmi, G R Duckwiler and Y P Gobin

AJNR Am J Neuroradiol 1996, 17 (2) 271-279
http://www.ajnr.org/content/17/2/271

Laboratory Simulations and Training in Endovascular Embolotherapy with a Swine Arteriovenous Malformation Model

Tarik F. Massoud, Cheng Ji, Fernando Viñuela, Francis Turjman, Guido Guglielmi, Gary R. Duckwiler, and Y. Pierre Gobin

Summary: We assessed the suitability of a swine experimental arteriovenous malformation model for laboratory simulations and training in endovascular embolotherapy. Embolizations with liquid glue or particles were performed in 10 animals. The parameters of injection (microcatheter position, concentration and volume of embolic agent, injection rate) were deliberately varied to simulate results that may be observed in clinical practice. A range of successful and less desirable therapeutic outcomes or complications was simulated. In one model, intravascular mean blood pressure in the "terminal feeder" rose after "nidus" embolization, consistent with observations in feeders of cerebral arteriovenous malformations. Experience in the technical aspects of embolotherapy was gained by repeated performances using this model. Simplicity of creation, clear angiographic visibility of feeders, a nidus and a draining vein, and hemodynamic similarities with cerebral arteriovenous malformations make this an attractive in vivo experimental model for learning the principles of embolotherapy, testing new embolic agents, and training/gaining experience in embolization techniques.

Index terms: Animal studies; Arteriovenous malformations, embolization; Interventional neuroradiology, models

Cerebral arteriovenous malformations (AVMs) are inherently dangerous lesions, occurring in a young age group in which hemorrhage, convulsions, or headaches can be severely debilitating or fatal (1). Therefore, an aggressive therapeutic approach generally is adopted in these patients. Endovascular embolization of AVMs has evolved over the last 2 decades into the most useful adjuvant therapeutic technique to conventional surgery. This evolution mostly is a reflection of advances in catheter technology, embolic materials, and the increasing experience acquired by interventional neuroradiologists.

Despite the increasing acceptance and use of embolotherapy in the management of AVMs, there remains a degree of inherent risk (of transient or permanent neurologic deficit, or death) related to this procedure. This risk is mostly attributable to the present lack of embolic agents possessing "ideal" properties (2), the complexity of cerebral AVMs and their blood supply, and the particular vulnerability of the surrounding brain. Complications of endovascular embolotherapy fall into two categories: (*a*) those attributable to technical mishaps, such as gluing of the microcatheter in an AVM feeder, vasospasm, dissection or rupture of an intracranial artery, dissection of neck vessels, and intracranial emboli from coaxial catheters in the neck; and (*b*) those consequent to the embolization process itself; namely, postembolization cerebral ischemia, intracranial hemorrhage, and vasogenic edema (3). Thus, extensive operator training and experience are required for the safe and effective use of embolic agents because of these great potential risks.

To date, training in AVM embolization procedures has been hindered by the lack of a suitable laboratory animal model. Recently, Massoud et al (4) have developed an experimental AVM model, with a nidus fashioned from bilateral carotid retia mirabilia of the swine. In this study, we evaluated the suitability of this model for in vivo simulation of endovascular embolotherapy.

Methods

All animal experimentation was conducted in accordance with policies set by the local university chancellor's animal research committee and National Institutes of Health guidelines. Ten Red Duroc swine were used in this study. The animals were 3 to 4 months old, weighed 30 to

Received October 21, 1994; accepted after revision May 18, 1995.

Presented at the 32nd Annual Meeting of the American Society of Neuroradiology, Nashville, Tenn, May 3–7, 1994.

From the Department of Radiological Sciences, University of California at Los Angeles.

Address reprint requests to Tarik F. Massoud, MD, Endovascular Therapy Service, Department of Radiological Sciences, UCLA Medical Center, 10833 Le Conte Ave, Los Angeles, CA 90024.

AJNR 17:271–279, Feb 1996 0195-6108/96/1702–0271

40 kg, were of mixed sex, and were maintained on a standard laboratory diet. After an overnight fast, each swine was premedicated with intramuscular 20 mg/kg of ketamine and 2 mg/kg of xylazine. General anesthesia was maintained with mechanical ventilation and inhalation of 1% to 2% halothane after endotracheal intubation.

AVM Construction and Preembolization Assessment

The relevant vascular anatomy of the swine head and neck and details of constructing the AVM model have been described previously (4). Briefly, preoperative endovascular occlusion of the right occipital artery, the muscular branch of the right ascending pharyngeal artery, and the right external carotid artery was performed to maximize postoperative blood channeling from both retia to the fistula. This procedure was followed by surgical formation of a side-to-side arteriovenous fistula between the right common carotid artery and the external jugular vein.

Immediate postoperative angiography was performed in all swine to demonstrate the AVM. Via the transfemoral route, a 6F Royal Flush guiding catheter (Cook, Bloomington, Ind) was positioned in the left common carotid artery. Nonionic contrast medium (6 mL) was injected to outline the three feeding arteries (left ascending pharyngeal artery, left ramus anastomoticus, and left arteria anastomotica), the nidus (bilateral retia mirabilia), and the draining vein (right ascending pharyngeal artery and right common carotid artery down to the fistula) (Fig 1). The rapid transit of blood from the left to the right side of the neck, across bilateral retia, was seen on rapid-sequence (up to 30 frames per second) digital subtraction imaging. Next, superselective angiograms were obtained via each of the three feeding arteries to demonstrate their relative contributions to filling of the nidus before its embolization. For the left ascending pharyngeal arteriogram, a Tracker 18 microcatheter/Seeker 14 microguidewire combination (Target Therapeutics, Fremont, Calif) or a flow-directed Magic 1.5 or 1.8 microcatheter (Balt, Montmorency, France) was coaxially navigated via the guiding catheter and positioned in the ascending pharyngeal artery just proximal to the left rete. Contrast medium (2 mL) was injected in this artery (Fig 2). For angiograms of both the left ramus anastomoticus and the left arteria anastomotica, a Tracker 10 microcatheter (Target Therapeutics, Fremont, Calif) was used, followed by injection of 1 mL of contrast medium.

In three swine, regional intravascular blood pressure measurements were made in the left ascending pharyngeal artery before AVM construction, and in components of the AVM (the right and left ascending pharyngeal arteries at the carotid-jugular fistula) after construction. The measurements on the venous side of the AVM model were obtained through an inflated balloon catheter placed in the proximal right common carotid artery (caudad to the fistula), before ligation or permanent balloon occlusion of the proximal right common carotid artery (4). In one swine, pressure in the main feeder of the AVM after particulate embolization also was assessed. Measurements were made through a microcatheter connected to a Hewlett-Packard 78205D pressure monitor with a Spectramed TNF-R pressure transducer (Spectramed, Oxnard, Calif).

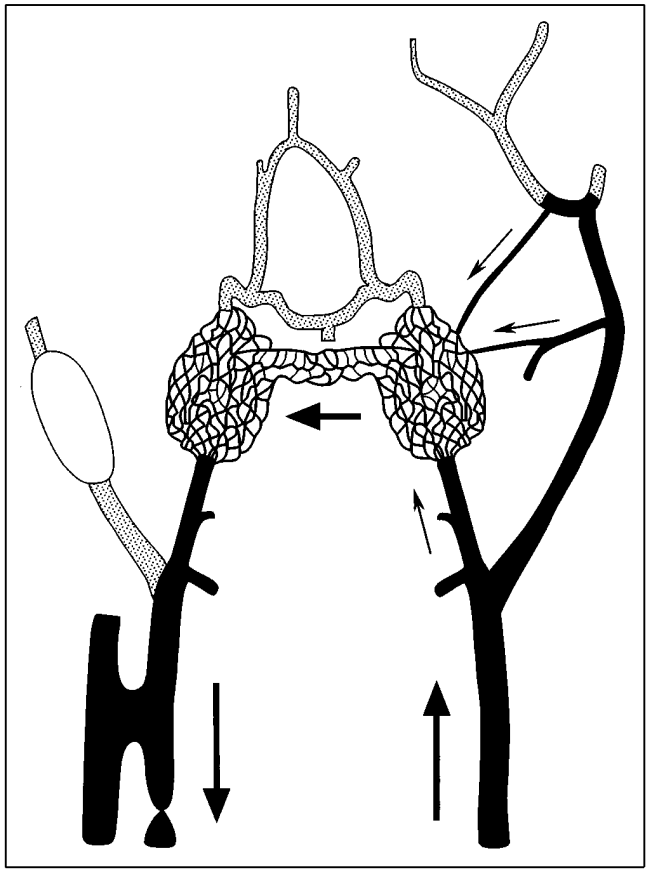

Fig 1. Schematic diagram of the AVM model. Main components of the AVM are in *black*. *Arrows* show direction of flow: from the left common carotid artery to both retia mirabilia (nidus) via the three feeding arteries (ie, left ascending pharyngeal artery, left ramus anastomoticus, and left arteria anastomotica), and retrograde down the right ascending pharyngeal artery toward the right carotid-jugular fistula. Note balloon inflated in the right external carotid artery.

AVM Embolization

Seven AVMs were embolized endovascularly with liquid glue (*N*-butyl 2-cyanoacrylate [NBCA]), and two with embolic particles (collagen microbeads). In an additional AVM, a combination of collagen microbeads to occlude the nidus and a platinum microcoil in a minor feeder was used. All embolizations were performed in AVMs immediately after their construction; no chronic models were used in this study. Two swine with mostly complete nidus occlusion were followed for 1 week after embolization and repeat common carotid and vertebral angiograms performed.

Embolization procedures using NBCA were performed in a standard fashion (5, 6). Ethiodized oil (Ethiodol, Sav-

Fig 2. Superselective angiogram via the left ascending pharyngeal (terminal feeder) artery demonstrates detail of the AVM nidus before embolization.

age, Meville, NY) was mixed with NBCA and tantalum powder in a clean metal container previously rinsed with 5% dextrose solution. For each procedure, 0.5 mL of NBCA was used in this preparation, to which was added a volume of ethiodized oil varying from 0.5 mL to 1.5 mL. Thus, two AVMs were embolized with mixtures at a 1:1 ratio of ethiodized oil to NBCA, two with mixtures at a 2:1 ratio, and three with mixtures at a 3:1 ratio. Tantalum powder (0.25 to 0.5 g) was added to each of these mixtures. Glacial acetic acid (30 μg) also was added to one of the mixtures (at a 1:1 ratio) before injection to delay its polymerization time (7). With the microcatheter positioned superselectively in the desired feeder, a preembolization flush injection of 5% dextrose was performed. The embolic mixture was then injected as a bolus and flushed into the vessel with a chaser bolus of 5% dextrose. The volume of embolic mixture injected in each AVM varied from 0.1 mL to 0.5 mL. Furthermore, the speed at which each mixture was pushed toward the nidus was subjectively tailored to the speed of blood flow on preembolization angiograms. The embolization was monitored fluoroscopically or recorded on rapid-sequence angiograms (up to 30 frames per second). In most procedures, the microcatheter was pulled out immediately after embolization to avoid adherence to the artery. When it was left in place, a postembolization superselective angiogram was performed to assess the extent of vascular occlusion. Further assessment of possible residual nidus supply was performed by contrast injection via the guiding catheter placed in the common carotid artery.

Embolization using collagen microbeads ($\approx$ 300 μm) was described previously by Turjman et al ("Collagen Microbeads: Experimental Evaluation of a New Embolic Agent in Swine," presented at the 32nd Annual Meeting of the American Society of Neuroradiology, Nashville, Tenn, May 3–7, 1994). A suspension of particles was diluted by mixing with contrast agent and saline. Embolization was performed via the microcatheter placed superselectively in the desired feeder. A slow injection of 0.5 mL of the dilute particle suspension was done under fluoroscopic digital subtraction imaging until complete contrast stasis was achieved in the distal feeder and proximal nidus. Careful angiographic monitoring of the extent of nidus or feeder occlusion was necessary and the speed of injection adjusted to produce satisfactory embolization without particle reflux (8). In one AVM, embolization via the terminal feeder was supplemented with further particle injection and release of a platinum microcoil (Target Therapeutics, Fremont, Calif) in an en passage feeder (left ramus anastomoticus). Postembolization angiograms were obtained similarly via the superselective microcatheter and/or the common carotid artery guiding catheter.

Results

All swine tolerated the general anesthesia and surgical and endovascular procedures with no ill effects. All AVM models were created successfully, resulting in clear angiographic demonstration of a terminal feeder and two en passage feeders supplying a nidus in each model. In one swine, anatomic variants in the arterial supply of the left rete mirabile were noted, where both ramus anastomoticus and arteria anastomotica consisted of several tiny branches. This precluded approach to the nidus and embolization via these en passage feeders.

Intravascular pressure measurements in the normal left ascending pharyngeal arteries of three swine (before AVM construction) showed an average mean blood pressure of 77 mm Hg. Mean pressure in the same artery after AVM construction (ie, the terminal feeder) dropped to an average of 67 mm Hg. Mean intravascular pressure in the right ascending pharyngeal artery after AVM construction (ie, the draining vein) dropped even further to an average of 46 mm Hg, because of the presence of the ipsilateral carotid-jugular fistula. Mean blood pressure on the common carotid artery side of the carotid-jugular fistula averaged 22 mm Hg.

Injection of NBCA in the AVM feeders resulted in a variable extent of vascular occlusion, which depended on the parameters of embolization. Thus, it was possible to simulate a range of desirable and undesirable results of AVM embolization as may be observed in clinical practice. Complete occlusion of most of the nidus was achieved by using about 0.2 to 0.3 mL of ethiodized oil and NBCA mixtures with a volume ratio of 3:1, injected via the terminal feeder (Fig 3). Injection in this terminal feeder of smaller volumes and/or more concentrated

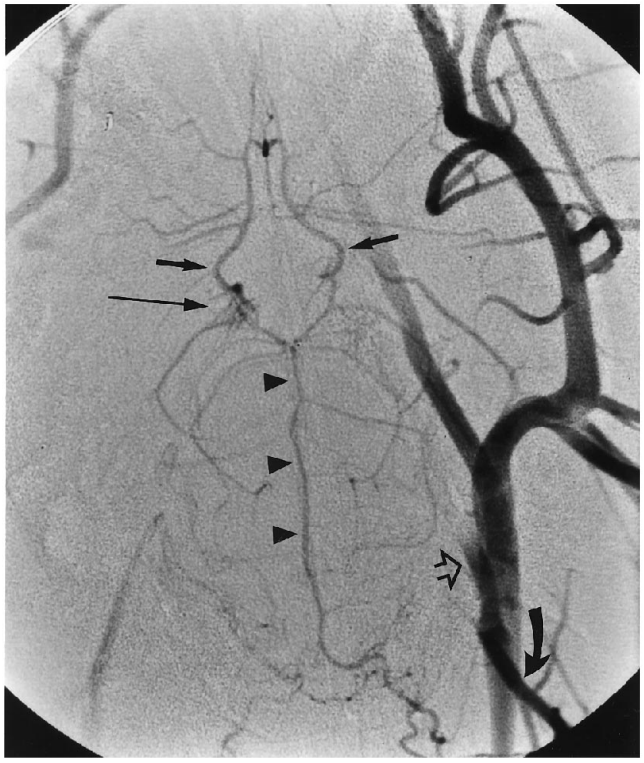

Fig 3. Left common carotid arteriogram after glue injection via the terminal feeder. Most of the AVM nidus is occluded. There is some retrograde filling of the right rete (*long arrow*) from the circle of Willis. Note cast of glue in the left ascending pharyngeal artery (*open arrow*) caused by reflux down to, but not including, the origin of the left occipital artery (*curved arrow*). The basilar artery (*arrowheads*) now supplies the circle of Willis (*short arrows*).

Fig 4. Left external carotid arteriogram after glue occlusion of the distal terminal feeder, proximal left rete, and midline retial vessels only. Now the two en passage feeders (ramus anastomoticus [*curved arrow*] from the middle meningeal artery [*small arrows*], and arteria anastomotica [*open arrow*]) supply an incompletely embolized nidus (patent distal left rete [*long arrow*]) from the external carotid system.

glue resulted in unsatisfactory occlusion of the distal terminal feeder and proximal left rete only, with persistent filling of the nidus through the patent en passage feeders (Fig 4). On the other hand, injections of larger volumes or more dilute glue resulted in some further penetration and occlusion of the nidus, but also in undesirable reflux of embolic agent down the terminal feeder (especially after excessively fast injections) (Fig 5). This observed untoward effect of glue reflux down the left ascending pharyngeal artery was considered significant if the reflux reached and occluded the muscular branch of the left ascending pharyngeal artery (ie, simulating occlusion of a human arterial branch supplying adjacent normal brain, off an AVM feeder). If the reflux reached and occluded the more proximal and much larger occipital artery, then the complication was considered serious. Superselective catheterization of either the left arteria anastomotica or the left ramus anastomoticus was attempted in two swine for glue embolization and in another swine for particle embolization. However, a secure position of the microcatheter tip to allow safe embolization in the desired artery could not be achieved. In one swine, therefore, glue embolization of the nidus via the left ramus anastmoticus was attempted with a mixture containing acetic acid. Because the tip of the microcatheter could not be secured in the orifice of the ramus anastomoticus, most of the injected glue entered the left middle meningeal artery (again, simulating untoward embolization of a normal brain artery). Delayed polymerization, however, did allow a minimal amount of glue to reach the left rete. The two swine maintained for 1 week after NBCA occlusion of most of the nidus demonstrated no adverse clinical sequelae during this period, and follow-up angiography showed compensatory enlargement of the basilar artery supplying the circle of Willis.

Embolization with collagen particles via the terminal feeder resulted in near total occlusion of the left rete (and, therefore, nonfilling of almost all the nidus) in one swine (Fig 6). Intra-

5

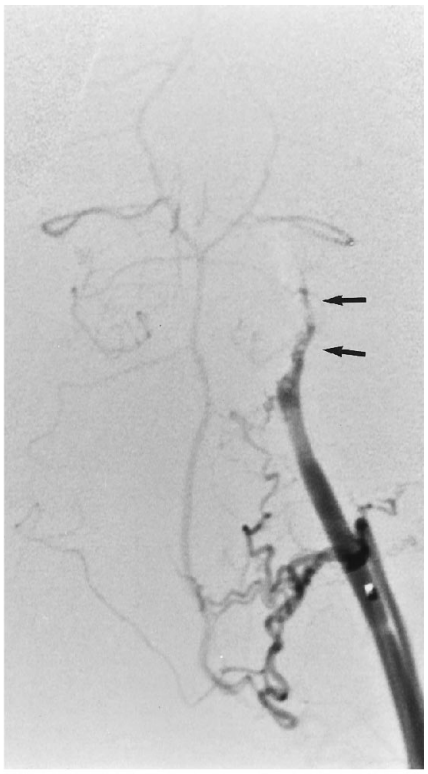

6

Fig 5. Left common arteriogram after glue injection via the terminal feeder. Only the proximal half of the left rete is occluded, and there is reflux of glue down to, but not including, the muscular branch of the left ascending pharyngeal artery (*short arrow*). There is persistent filling of the distal left rete (*long arrow*) via en passage feeders.

Fig 6. Superselective arteriogram via the terminal feeder after embolization of the AVM with particles. There is near total occlusion of the left rete (arrows).

vascular blood pressure in the terminal feeder of this swine rose gradually from a preembolization mean of 48 mm Hg to 74 mm Hg after partial occlusion of the nidus, consistent with observations in human AVMs (9). In a second swine, only the proximal nidus and distal feeder were satisfactorily embolized, resulting in persistent supply of the rest of the nidus by the two en passage feeders. In the third swine, the first injection in the terminal feeder was performed with a relatively high concentration of particles, resulting in unsatisfactory immediate occlusion just at the entrance to the nidus. Therefore, further embolization of the AVM nidus was undertaken after catheterization of the left middle meningeal artery for approach to the left ramus anastomoticus (Fig 7A through D). In this position, a more dilute particle solution was injected. A short platinum microcoil also was released in the ramus anastomoticus. This combination resulted in progressive occlusion of the AVM nidus and its en passage feeder but also resulted in an occluded middle meningeal artery (a simulated complication, as above). Nidus supply from the left arteria anastomotica was not observed on further angiograms.

Discussion

Animal laboratories have been used for many years in the teaching of skills and procedures necessary for safe and effective clinical practice. An ongoing laboratory may be of benefit by: (*a*) establishing and improving physician-in-training ability and confidence in new, complex, or risky procedures; (*b*) maintaining these acquired skills through repeated simulated performances at times when they are not being used in clinical practice; and (*c*) providing a springboard for related research studies (10). Many in vivo laboratory models of human intracranial vasculopathies have been used in the past for training in interventional neuroradiologic procedures. These simulators (ie, teaching "machines" [11]) are of value, because complex therapeutic tasks must be learned when they are potentially dangerous either to the operator or subject, and the cost of failure may be high (11). Animal experimental models of intracranial aneurysms (12–14) and simple arteriovenous fistulas (15–17) have been available commonly as tools for laboratory training in neuroendovascular occlusion therapies. These models are possible because of the rela-

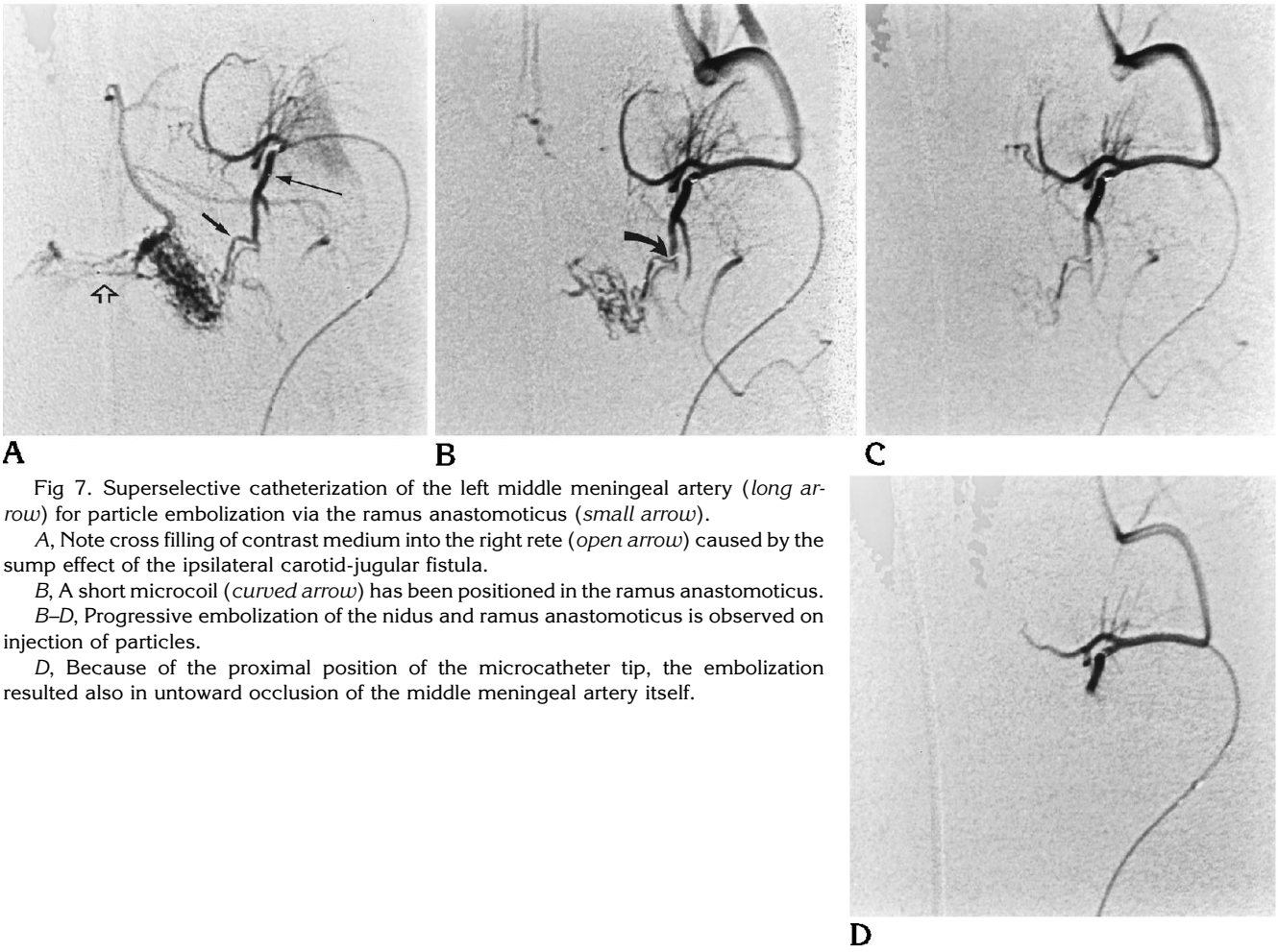

Fig 7. Superselective catheterization of the left middle meningeal artery (*long arrow*) for particle embolization via the ramus anastomoticus (*small arrow*).

A, Note cross filling of contrast medium into the right rete (*open arrow*) caused by the sump effect of the ipsilateral carotid-jugular fistula.

B, A short microcoil (*curved arrow*) has been positioned in the ramus anastomoticus.

B–D, Progressive embolization of the nidus and ramus anastomoticus is observed on injection of particles.

D, Because of the proximal position of the microcatheter tip, the embolization resulted also in untoward occlusion of the middle meningeal artery itself.

tively simple and easily modeled morphologic and hemodynamic features of these vasculopathies, as compared with AVMs.

To date, training in endovascular embolization of cerebral AVMs has been hampered by the lack of a suitable laboratory animal model. To address this deficiency, various mathematical/computer models, in vitro models, and useful but incompletely representative in vivo models have been used in attempts to simulate in experimental settings the theoretical and/or practical processes occurring during embolization of an AVM. Thus, Hecht et al (18) have computer modeled the hemodynamics of an AVM nidus during particulate embolization. Their theoretical analysis helped provide an understanding for the apparent incremental flow reduction seen during use of particulate agents. In vitro simulators of endovascular embolotherapy have been available since the early days of interventional neuroradiology, thanks mainly to the works of Kerber and colleagues (11, 15). They used pump-driven fluid circuits of clear plastic tubing in configurations that simulate the abnormal vascular morphology of AVMs. These models were subsequently used for refining endovascular devices and as teaching and research simulators for embolotherapy, allowing for the laboratory practice of endovascular techniques under safe and stress-free conditions. More recent in vitro modeling has involved the placement within similar fluid circuits of added components that more closely resemble an AVM nidus, such as polymer sponges of varying pore size (Kerber CW, Hecht ST, "AVM Models for MRA and Endovascular Therapy," presented at the 32nd Annual Meeting of the American Society of Neuroradiology, Nashville, Tenn, May 3–7, 1994). In one model, an AVM nidus was simulated by use of plastic mesh encased by a plastic bag and covered in watertight silicone sealant (19). In another simulator,

a hydraulic model was constructed from silicone and glass tubes of different internal diameters; the nidus consisted of ten tubules arranged in parallel (20). Despite their low cost and ease of manufacture, all these in vitro models have the drawback of demonstrating only the very general principles of embolization techniques and/or the physical occlusive characteristics of embolic materials. Furthermore, none of them possesses viable vascular endothelium and circulating whole blood, both of which have a significant influence on intravascular events during the embolization process.

In comparison with in vitro models, the use of animal AVM models would represent a significant step forward in the accurate simulation of human endovascular embotherapy. In addition to the specific provision of vascular endothelium and circulating whole blood, these models would possess biological behavior and offer biovariability traits unavailable in mathematical or plastic models (21). Therefore, in vivo models are much more realistic representations of human AVMs, which also would allow their use as more meaningful simulators for endovascular embolization. Previous attempts at in vivo simulation of embolotherapy have centered either on the use of the normal swine carotid rete mirabile (as a morphologic replica of an AVM nidus) (5, 22, 23) or on normal animal peripheral vessels (mainly for studying the polymerization characteristics of liquid embolic agents) (6). However, none of these models accurately mimicked a true human AVM because of the lack of rapid arteriovenous shunting through a nidus (ie, the morphologic and hemodynamic hallmark of these lesions).

To address the shortfalls of previous laboratory animal simulators for embolotherapy, we developed an animal model of an AVM with closer resemblance to human lesions than available previously. The model still makes use of the carotid rete mirabile of swine, but with the added experimentally induced feature of faster blood flow through bilateral retia. Shunting of blood across both retia, from one side of the neck to the other, is produced by surgical formation of a large unilateral carotid-jugular fistula, and is facilitated by presurgical endovascular occlusion of several arteries ipsilateral to the fistula. This rapid circulatory diversion results in clear angiographic visualization of a main terminal feeder (the left ascending pharyngeal artery), two minor en passage feeders (left ramus anastomoticus and left arteria anastomotica), a nidus (bilateral retia mirabilia), and a draining vein (the right ascending pharyngeal artery and segment of right common carotid artery above the fistula). Intravascular blood pressure measurements within components of this model confirm the presence of a pressure gradient (of about 20 mm Hg) between the main terminal feeder and the draining vein (across the nidus), a feature unavailable in previous experimental simulations of embolotherapy using the normal rete mirabile. Furthermore, histopathologic studies of the nidus in chronically maintained models (up to 8 weeks old) demonstrate striking transformations in the rete microvasculature (Massoud TF, Vinters HV, Ji C, et al, "An Experimental Chronic Arteriovenous Malformation Model in Swine: Light Microscopy and Angiographic Follow-up," presented at the Symposium Neuroradiologicum, Japan, October 1994), including attenuation of the internal elastic lamina and intimal cushions, features akin to those of human AVMs. Therefore, the gross morphologic, histopathologic, angiographic, and hemodynamic features of this AVM model lend support to its suitability as a laboratory simulator for endovascular embolotherapy.

As with training in other invasive medical specialities (eg, surgery, interventional cardiology, interventional radiology), training in neuroendovascular therapy should require the development of two broad types of skills, cognitive and technical (24). The use of our laboratory AVM simulator has proved to be a very useful tool in helping trainees acquire both sets of skills. The cognitive skills necessary for the purpose of treating cerebral AVMs by the endovascular approach include a full understanding of the anatomic and pathophysiologic characteristics of these lesions and their implications, particularly the presence of shunting flow through a low resistance abnormal vascular network, and the presence of vulnerable normal territories (that are potentially harmed by the embolization process) in the surroundings of AVMs. Furthermore, knowledge of the principles of embolotherapy, and how these may be adapted to specific morphologic and hemodynamic characteristics of AVMs, is required. Thus, the necessity to occlude all of the AVM nidus while avoiding less desirable outcomes or complications (such as partial nidus obliteration resulting in persistent supply by other patent

feeders and extranidal occlusion of feeders and/or other arteries supplying normal territories) and periembolization hemodynamic changes within components of the AVM can be appreciated by embolization procedures in this in vivo model. Of note, however, is the presence in this model of both normal internal carotid arteries emerging from the nidus—a shortfall in terms of complete morphologic replication of a human AVM (4). Because of the presence of these arteries, the disastrous complication of AVM nidus rupture attributable to draining vein occlusion with glue cannot be simulated. Whereas it may be possible for injected glue to reach the draining vein (by prolonging the polymerization time of the glue), this will not lead to nidus rupture, because the resultant intranidal hypertension is disseminated via both internal carotid arteries. If anything, these two arteries also act as draining veins in that they are efferent to the nidus. Although they do not behave hemodynamically as draining veins (because they lead to a downstream intracranial capillary system), their presence adds to the morphologic complexity of the AVM model and the realism of the embolotherapy simulation, because it is necessary also to avoid their occlusion during embolic agent injection. It has to be said, nevertheless, that both retia mirabilia act as a large anastomotic bed of microvessels that mimic a purely plexiform AVM nidus. In this model, there is no replication of the large (greater than 1 mm in diameter) fistulous components that are seen particularly in large and giant brain AVMs. These fistulas have a significant influence on the overall strategies in delivery of the embolic agent, its permeation of the nidus, and its potential spread to the draining veins. Therefore, the relative uniformity of the size of the retia microvessels allows the use of this model to simulate embolotherapy of some brain AVMs and provides an overall good initial experience with the use of embolic material in the presence of arteriovenous shunting.

The technical skills that may be mastered by simulating embolotherapy in this model are numerous. Thus, an appreciation may be obtained for the types and performance characteristics of currently available equipment, including conventional guiding catheters and guidewires, microcatheters, and microguidewires (25). The strategies and techniques of selective and superselective angiography (26) of an AVM can be learned in this morphologically realistic model. The use of microcatheters for obtaining intravascular pressure measurements also can be appreciated in a hemodynamically realistic setting. As applicable to human AVMs, several methods of vessel occlusion can be practiced in this embolotherapy simulator. In this study, we have used liquid and particulate embolic agents to occlude the AVM nidus (as is most often done in clinical practice), as well as microcoils to occlude feeders. In addition, the construction of the AVM model itself necessitates the use of detachable balloons, microcoils, or endovascular electrothrombosis as occlusive techniques in large vessels. The use of all these devices/techniques helps the trainee to recognize their behavior, limitations, and potential complications in morphologically and hemodynamically realistic vascular trees, under safe and stress-free conditions. In particular, the (potentially risky) intravascular delivery of appropriately concentrated NBCA, at the correct injection speed, and in the safest position within an arterial feeder can be learned in an in vivo simulator possessing an experimental fast-flowing nidus. An added advantage of this AVM model is that embolic occlusion of both retia mirabilia in the swine appears possible without demise of the animal because of adequate circulatory compensation via the posterior circulation. Therefore, the follow-up of embolized experimental AVMs and the temporal study of new embolic agents in a realistic setting may be possible with this model. Acute AVM models (as used in this study) are adequate for simple training in embolotherapy, but chronic models (with their underlying induced histologic transformations) would be more suitable when the main interest is studying the histologic effects and temporal behavior of the embolic agent in question. Lastly, confidence and experience in the technical aspects of AVM embolotherapy may be gained by repeated performances using this model.

In conclusion, we have demonstrated the suitability of a swine AVM model as a laboratory simulator for endovascular embolotherapy. Simplicity of creation, and clear visibility of feeders, a fast-flowing nidus, and a draining vessel, make this an attractive model for learning the principles of embolotherapy, testing new embolic agents, and training or gaining experience in embolization techniques.

Acknowledgments

We are grateful to John Robert and Roger C. McGath for their technical assistance in conducting this research at the Leo G. Rigler Radiological Research Center.

References

1. Stein BM. Surgical decisions in vascular malformations of the brain. In: Barnett JM, Mohr JP, Stein BM, Yatsu FM, eds. *Stroke: Pathophysiology, Diagnosis, and Management*. New York, NY: Churchill Livingstone; 1992:1093–1133
2. Graves VB, Duff TA. Intracranial arteriovenous malformations: current imaging and treatment. *Invest Radiol* 1990;25:952–960
3. Viñuela F, Fox AJ. Interventional neuroradiology. In: Barnett JM, Mohr JP, Stein BM, Yatsu FM, eds. *Stroke: Pathophysiology, Diagnosis, and Management*. New York, NY: Churchill Livingstone 1992:1145–1167
4. Massoud TF, Ji C, Viñuela F, et al. An experimental arteriovenous malformation model in swine: anatomic basis and construction technique. *AJNR Am J Neuroradiol* 1994;15:1537–1545
5. Brothers MF, Kaufmann JCE, Fox A, et al. N-butyl 2-cyanoacrylate, substitute for IBCA in interventional neuroradiology: histopathologic and polymerization time studies. *AJNR Am J Neuroradiology* 1989;10:777–786
6. Wildus DM, Lammert GK, Brant A, et al. In vivo evaluation of iophendylate-cyanoacrylate mixtures. *Radiology* 1992;185:269–273
7. Spiegel SM, Viñuela F, Goldwasser MJ, et al. Adjusting polymerization time of isobutyl-2-cyanoacrylate. *AJNR Am J Neuroradiology* 1986;7:109–112
8. Kerber CW. Flow-controlled therapeutic embolization: a physiologic and safe technique. *AJNR Am J Neuroradiology* 1980;1:77–81
9. Duckwiler GR, Dion J, Viñuela F, et al. Intravascular microcatheter pressure monitoring: experimental results and early clinical evaluation. *AJNR Am J Neuroradiology* 1990;11:169–175
10. Olshaker JS, Brown CK, Arthur DC, et al. Animal procedure laboratory surveys: use of the animal laboratory to improve physician confidence and ability. *J Emerg Med* 1989;7:593–597
11. Kerber CW, Flaherty LW. A teaching and research simulator for therapeutic embolization. *AJNR Am J Neuroradiology* 1980;1:167–169
12. Geremia GK, Hoile RD, Haklin MF, et al. Balloon embolization of experimentally created aneurysms: an animal training model. *AJNR Am J Neuroradiol* 1990;11:659–662
13. Guglielmi G, Ji C, Massoud TF, et al. Experimental saccular aneurysms, II: a new model in swine. *Neuroradiology* 1994;36:547–550
14. Massoud TF, Guglielmi G, Ji C, et al. Experimental saccular aneurysms, I: a review of surgically constructed models and their laboratory applications. *Neuroradiology* 1994;36:537–546
15. Kerber CW. Experimental arteriovenous fistula: creation and percutaneous catheter obstruction with cyanoacrylate. *Invest Radiol* 1975;10:10–17
16. Kerber CW, Bank WO, Comwell LD. Calibrated leak balloon microcatheter: a device for arterial exploration and occlusive therapy. *AJR Am J Roentgenol* 1979;132:207–212
17. Anderson JH, Wallace S, Gianturco C. Transcatheter intravascular coil occlusion of experimental arteriovenous fistulas. *AJR Am J Roentgenol* 1977;129:795–798
18. Hecht ST, Horton JA, Kerber CW. Hemodynamics of the central nervous system arteriovenous malformation nidus during particulate embolization: computer model. *Neuroradiology* 1991;33:62–64
19. Bartynski WS, O'Reilly GV, Forrest MD. High-flow-rate arteriovenous malformation model for simulated therapeutic embolization. *Radiology* 1988;167:419–421
20. Nagasawa S, Kawanishi M, Tanaka H, et al. Hemodynamic study of arteriovenous malformations using a hydraulic model. *Neurol Res* 1993;15:409–412
21. Cheong J. The use of animals in medical education: a question of necessity vs. desirability. *Theor Med* 1989;10:53–57
22. Lee DH, Wriedt CH, Kaufmann JCE, et al. Evaluation of three embolic agents in pig rete. *AJNR Am J Neuroradiol* 1989;10:773–776
23. Lylyk P, Viñuela F, Vinters HV, et al. Use of a new mixture for embolization of intracranial vascular malformations: preliminary experimental experience. *Neuroradiology* 1990;32:304–310
24. Cowley MJ, Faxon DP, Holmes DR. Guidelines for training, credentialing, and maintenance of competence for the performance of coronary angioplasty. *Cathet Cardiovasc Diag* 1993;30:1–4
25. Dion JE. Principles and methodology. In: Viñuela F, Halbach VV, Dion J, eds. *Interventional Neuroradiology: Endovascular Therapy of the Central Nervous System*. New York, NY: Raven Press 1992:1–15
26. Viñuela F, Fox AJ, Debrun G, et al. Preembolization superselective angiography: role in the treatment of brain arteriovenous malformations with isobutyl-2 cyanoacrylate. *AJNR Am J Neuroradiol* 1984;5:765–769